Published in final edited form as:
Clin Cancer Res. 2012 February 1; 18(3): 771–782. doi:10.1158/1078-0432.CCR-11-1916.

Omental adipose tissue-derived stromal cells promote vascularization and growth of endometrial tumors

Ann H. Klopp[1], **Yan Zhang**[2], **Travis Solley**[1], **Felipe Amaya-Manzanares**[2], **Frank Marini**[3], **Michael Andreeff**[3], **Bisrat Debeb**[1], **Wendy Woodward**[1], **Rosemarie Schmandt**[4], **Russell Broaddus**, **Karen Lu**[4], and **Mikhail G. Kolonin**[2,*]

[1]Department of Radiation Oncology, The University of Texas MD Anderson Cancer Center

[2]The Brown Foundation Institute of Molecular Medicine, The University of Texas Health Science Center at Houston

[3]Department of Leukemia, The University of Texas MD Anderson Cancer Center

[4]Department of Gynecologic Oncology, The University of Texas MD Anderson Cancer Center

[5]Department of Pathology, The University of Texas MD Anderson Cancer Center

Abstract

Purpose—Adipose tissue contains a population of tumor-tropic mesenchymal progenitors, termed adipose stromal cells (ASC), which engraft in neighboring tumors to form supportive tumor stroma. We hypothesized that intra-abdominal visceral adipose tissue may contain a uniquely tumor promoting population of ASC to account for the relationship between excess visceral adipose tissue and mortality of intra-abdominal cancers.

Experimental Design—To investigate this, we isolated and characterized ASC from intra-abdominal omental adipose tissue (O-ASC) and characterized their effects on endometrial cancer progression as compared to subcutaneous adipose derived mesenchymal stromal cells (SC-ASC), bone marrow derived mesenchymal stromal cells (BM-MSC) and lung fibroblasts. To model chronic recruitment of ASC by tumors, cells were injected metronomically into mice bearing Hec1a xenografts.

Results—O-ASC expressed cell surface markers characteristic of BM-MSC and differentiated into mesenchymal lineages. Co-culture with O-ASC increased endometrial cancer cell proliferation in-vitro. Tumor tropism of O-ASC and SC-ASC for human Hec1a endometrial tumor xenografts was comparable, but O-ASC more potently promoted tumor growth. Compared with tumors in SC-ASC-injected mice, tumors in O-ASC-injected mice contained higher numbers of large tortuous desmin-positive blood vessels, which correlated with decreased central tumor necrosis and increased tumor cell proliferation. O-ASC-exhibited enhanced motility as compared to SC-ASC in response to Hec1a secreted factors.

Conclusions—Visceral adipose contains a population of multipotent MSC that promote endometrial tumor growth more potently than MSC from subcutaneous adipose tissue. We propose that O-ASC recruited to tumors express specific factors that enhance tumor vascularization, promoting survival and proliferation of tumor cells.

[*]Corresponding author: Mikhail Kolonin, Ph.D., John S. Dunn Research Scholar, Associate Professor, Institute of Molecular Medicine, Center for Stem Cell and Regenerative Medicine, University of Texas Health Science Center at Houston, 1825 Pressler St., Rm. 630-G, Houston, TX 77030, Office: 713-500-3146.

Introduction

Endometrial cancer is the most common gynecologic malignancy in the United States and is strongly linked with obesity (1, 2). Women with a body mass index (BMI, calculated as kg/m^2) greater than 40 have a greater than 6 fold relative risk of death from uterine cancer than lean women (2, 3). Furthermore, estimates suggest that 39% of cases of endometrial cancer can be attributed to obesity (4). The relationship between obesity and endometrial cancer has generally been attributed to estrogen and other paracrine factors secreted by adipose tissue (5).

However, a more direct relationship between adipose tissue and malignant tumors is suggested by recent studies demonstrating that adipose tissue contains a population of mesenchymal progenitor cells that migrate into tumors and can facilitate tumor progression (6). These adipose stromal cells (ASC) have many features of bone marrow-derived mesenchymal stromal cells (BM-MSC), including cell surface marker expression, plastic adherence, and the capacity to differentiate into cells of mesenchymal lineage: osteoblasts, chondrocytes and adipocytes (7, 8). Accumulating evidence indicates that cancer-associated fibroblasts (CAF), which provide a trophic tumor microenvironment, are, at least to some extent, derived from MSC (9–13). MSC have been reported to impact tumor progression, increasing tumor initiation and promoting metastasis in some models (14–19). This evidence suggests that the strong link between obesity and endometrial cancer may be attributed, at least in part, to increased availability of adipose stromal cells (ASC) which are recruited to form a supportive tumor microenvironment.

Excess intra-abdominal adipose tissue further increases the risk, and in some cases, mortality of intra-abdominal cancers such as prostate, colon, pancreatic, and endometrial cancer (3, 20, 21). We hypothesized that a tumor promoting population of multipotent mesenchymal stromal cells in visceral adipose tissue could explain this relationship. To investigate this, we isolated a population of ASC from the omentum, the major depot of visceral intra-abdominal adipose tissue. The effect of omental-derived ASC (O-ASC) was then compared to bone marrow derived MSC (BM-MSC), subcutaneous ASC (SC-ASC) and control fibroblasts by using ex vivo and in vivo assays.

Materials and Methods

Cell culture

Cells were grown in α-minimum essential medium (α-MEM) containing 20% fetal bovine serum (FBS), L-glutamine and penicillin–streptomycin. Hec1a and WI38 cells were obtained from American Type Culture Collection (Manassas, VA, USA). Hec1a cells were stably transfected using lipofectamine, with pEF-Luc. SC-ASC from a cancer-free female donor (BMI=33.0) were reported previously (22). Bone marrow MSC were isolated from normal individuals undergoing bone marrow harvest for allogeneic transplantation following informed consent, according to institutional guidelines under the approved protocol, as described previously (23). Briefly, mononuclear cells were separated by centrifugation over a Ficoll-Hypaque gradient (Sigma-Aldrich), suspended in α-MEM / 10% FBS, and plated on 180 cm^2 dishes. After 3 days, non-adherent cells were removed by washing with phosphate-buffered saline (PBS), and monolayers of adherent cells were cultured until they reached confluence. Cells were then trypsinized (0.25% trypsin with 0.1% EDTA) and subcultured at densities of 5,000–6,000 cells/cm^2. Cell passages 3–10 were used for the experiments (24). Cultured cells were routinely tested for viability with trypan blue exclusion and maintained high viability (>95%). For in vivo experiments, the minute fraction of dead cells was predominantly removed by washing prior to trypsinization. For flow cytometric analysis, cells were routinely pre-gated to exclude cell clumps,

contaminating polymorphonuclear cells, red blood cells, platelets, endothelial microparticles, debris, as well as dead cells based on 7-AAD staining.

Isolation of omental ASC

Under an IRB approved protocol, grossly normal appearing human omentum was obtained from the staging procedures. O-ASC1 were isolated from a patient (BMI=25.3) with recurrent adenocarcinoma of endometrium and ovary (omentum not involved). O-ASC2 were isolated from a patient (BMI=30.4) with recurrent granulosa cell tumor of the ovary (omentum involved). ASC were isolated according to published protocols (24). Tissue was subjected to mechanical disruption, followed by 0.5 mg/ml collagenase type I (Worthington Biochemical, Lakewood, NJ) and 50 U/ml dispase (Becton Dickinson, Franklin Lakes, NJ) digestion according to published protocols (6). Digested adipose tissue was centrifuged at 1000 rpm. Supernatant containing adipocytes was moved and cell pellet was resuspended in EGM-2MV (EBM-2 media with EGM-2MV growth factor supplementation from Lonza, Walkersville, MD). Resuspended cells were filtered through 100 μm cell strainer (Becton Dickinson, Franklin Lakes, NJ) and followed by 40μm cell strainer. Red blood cells were lysed using in 5 ml of RBC Lysis Buffer (eBioscience, San Diego, CA) with incubation in 37°C water bath for 10 minutes. Remaining mononuclear cells were resuspended and plated in EGM-2MV medium.

Characterization of O-ASC lines

After isolation, cells were expanded *in-vitro*, and then characterized with flow cytometry to evaluate cell surface marker expression. O-ASC1 was characterized at passage 3 and O-ASC2 at passage 5 with antibodies against the following markers: CD34, CD44, CD45, CD29, CD 90, EpCam (from Becton Dickinson, Franklin Lakes, NJ) and CD105 (from BioLegend, San Diego, CA). Cell differentiation studies were performed as described previously (25, 26). For osteoblast differentiation, confluent cells in 6 well plates were cultured in NH OsteoDiff Media (Miltenyi, Auburn, CA) for 3 weeks with the media changed 2 times a week. After 3 weeks media was removed, cells were washed 3 times with PBS and fixed with pre-cooled 100% methanol. Cells were stained with Alizarin Red S solution for 2–5 minutes at room temperature to visualize orange-red calcium deposits, or with von Kossa. For adipocyte differentiation, confluent cells in 6 well plate were cultured in adipogenic induction media, DMEM (Mediatech, Mannassas, VA) supplemented with 10% FBS, 1% Penicillin/Streptomycin, 10ug/ml Insulin, 500μM 3-isobutyl-1-methylxanthine (Sigma Aldrich, St. Louis, MO), 1 μM Dexamethasone (Sigma Aldrich, St. Louis, MO), and 200 μM Indomethacine (Sigma Aldrich, St. Louis, MO). After cells were maintained in induction media for 48–72 hours, media was changed to adipogenic maintenance media supplemented with 10% FBS, 1% Penicillin/Streptomycin, and 10ug/ml insulin for 24 hours. After 24 hours, media was changed back to induction media and cycle was repeated three times. After the third induction step, cells were in maintenance media for 10 days changing media twice a week. Cells were then fixed in 10% formalin for 1–2 hours followed by 60% isopropanol. Oil Red O (Sigma Aldrich, St. Louis, MO) stain was applied to visualize red lipid vacuoles. For chondrocyte differentiation, one million cells in a 15 ml conical were pelleted and resuspended in 2 ml of chondrocyte media; DMEM 1X (Mediatech, Mannassas, VA) supplemented with 1% Penicillin/Streptomycin, 50μg/ml Ascorbic Acid (Sigma Aldrich, St. Louis, MO), 100 nM Dexamethasone (Sigma Aldrich, St. Louis, MO) and 10 ng/ml TGF-β3 (Invitrogen, Camarillo, CA). Cells were then incubated under 5% CO_2 as a pellet at 37°C with cap loosened to allow for gas exchange. TGF-β3 was added daily to a concentration of 10 ng/ml. Media was changed 3 times a week for 21 days. Cell pellet was rinsed in PBS and fixed with Gendre's Fluid, after which paraffin-embedded blocks were sectioned and stained with antibodies against collagen II.

Proliferation Assay

Luciferase-labeled Hec1a cells were plated at a density of 1000 cells/well in a BD Falcon 96 well plate alone or in 1:1 co-culture with O-ASC1, O-ASC2, BM-MSC, SC-ASC, or WI38. Co-cultures were performed in either α-MEM (Mediatech, Manassas, VA) with 250 μg/ml G418. After 24 hours luciferase expression was measured in 0.15 mg/ml D-luciferin. After 1 hour incubation at 37°C, luminescence was measured with spectrophotometer (FLUOstar Omega, BMG Labtech, Offenburg, Germany). Media was then replaced and measurements were repeated every other day until cells reached confluence.

Generation of luciferase- GFP- and RFP-expressing cells

Cell lines were labeled with the green fluorescent protein (GFP) using a lentiviral vector, pFUGW (27) that was generously provided by Dr. Baltimore (Caltech). The titers of virus stocks were determined by calculating the percentage of GFP-positive (GFP^+) 293T cells transduced with serially diluted virus suspensions. For transduction, the O-ASC and SC-ASC cell lines were seeded at moderate density overnight. Two hours before transduction, the medium was changed, and then transductions were carried out for 24 h in the presence of 8 μg/mL polybrene (Sigma). The cells were then FACS sorted and further expanded for injections. The MSC were labeled similarly but with a red fluorescent protein (RFP) generously obtained from Tsien's lab (UCSD) that was cloned into pFUGW construct in place of GFP.

Migration Assay

Stromal cell migration including O-ASC, WI38, BM-MSC, and SC-ASC was assayed in conditioned media (CM) generated from Hec1a cells. CM was collected from a 6 well plate which was plated with 300,000 cells per well incubated in serum-free media for 48 hours Migration assays were performed in a 24 well transwell (Corning Inc., Corning, NY) with 8 uM pores. Conditioned media was placed in lower portion of transwell and cell lines of interest on the upper portion of transwell. All samples were assayed at least in quadruplicate. Twenty-four hours later the number of cell migrated to the bottom of the transwell was measured by staining membranes with Hema 3 Stat Pack (Thermo Fisher Scientific, Waltham, MA) and mechanically removing residual cells on upper membrane. The number of cells on the membrane was then quantitiated/HPF.

In-vivo studies

Animal experimentation was approved by the Animal Welfare Committee of the University of Texas. Ten-week-old mice NU/NU-foxn1^{nu} (Jackson Laboratory, USA) were injected subcutaneously with 1.5×10^6 Hec1a cells in 150 μl of PBS info the right flank (5 mice/group). WI38 fibroblasts, MSC, O-ASC2 and SC-ASC were grown in α-MEM containing 20% FBS, L-glutamine prior to injection. O-ASC1 were grown in either α-MEM containing 20% FBS or EGM-2MV. Starting the next day mice were injected with 1.5×10^5 corresponding cells (or PBS) every third day onto lower back, alternating the side of injection. Tumor size was measured with a caliper and volume was calculated as length × width^2 × 0.52. Before tumors reached 1 cm in size, mice were euthanized and tumors were recovered from anesthetized mice after heart perfusion with 10 mL PBS. Immunofluorescence on formalin-fixed paraffin-embedded tissue sections was performed after antigen retrieval, washing with 0.2% Triton X-100, blocking in Serum-Free Protein Block (DAKO), followed by incubation with primary antibodies (4°C, 12 h) and secondary antibodies (room temperature, 1 h) in PBS containing 0.05% Tween 20. The primary antibodies used were as follows: goat anti-GFP from GeneTex (1:100), rabbit anti-RFP from Abcam (1:100), rabbit anti-Ki67 from Thermo Scientific (1:200), rabbit (1:200) or goat (1:100) anti-CD31 from Santa Cruz Biotechnology, and rabbit anti-desmin from Abcam

(1:200). Secondary donkey FITC-conjugated (1:150) and Cy3-conjugated (1:300) IgG were from Jackson ImmunoResearch. Nuclei were stained with Hoechst 33258 (Invitrogen). Masson's Trichrome staining of tumor sections was performed at UTHealth histology CORE facility. Images were acquired with Olympus IX70 inverted fluorescence microscope / MagnaFire software.

To assess tumor composition, three random internal tumor field views proximal to the capsule were inspected for each tumor at 100× magnification. In each field views, the proportion of the area positive for necrosis (Mason's trichrome anuclear pink staining), proliferation (containing Ki-67+ cells), vascularization (containing CD31+ vessels), and mature vasculature (containing desmin+ vessels) was scored by two investigators blinded to the experimental group of the samples. Data were averaged from individual field views for each group.

Statistical Analysis was performed with unpaired Student's *t* test. Normal distribution of data was confirmed by the Kolmogorov-Smirnovtest.

Results

Characterization of omental ASC

Cells were isolated from omental adipose tissue of two patients with gynecologic cancer: one with localized adenocarcinoma of endometrium and ovary, the other with grandulosa cell tumor of the ovary infiltrating the omentum. Tissue was subjected to mechanical disruption, followed by collagenase and dispase digestion (6). Adipocytes were removed with centrifugation and remaining mononuclear cells were plated and cultured in standard MSC expansion conditions. Morphologically, O-ASC from patients 1 and 2 (O-ASC1 and O-ASC2) exhibited a mesenchymal phenotype, similar to that previously reported for BM-MSC and SC-ASC (Fig. 1A).

To characterize cell surface marker expression on O-ASC, we expanded O-ASC 1 and 2 and compared cell surface marker expression with flow cytometry to BM-MSC (Fig. 1B). O-ASC expressed CD29, CD44, CD73, CD90 and CD105, which are characteristically expressed on MSC (28, 29). BM-MSC expressed slightly higher levels of CD44 and CD105 than O-ASC while O-ASC expressed slightly higher levels of CD29 than BM-MSC. O-ASC were negative for an epithelial marker Epcam, a monocyte marker CD11b, as well as for CD34 and CD45. This excludes malignant, monocytic, and endothelial cells as a possible origin of O-ASC.

To test if O-ASC exhibit multipotency typical of MSC (7) *in-vitro*, we subjected them to differentiation assays (Supplementary Fig. S1). Upon adipogenic induction, O-ASC formed lipid droplets, which were detected with Oil Red O stain demonstrating lipogenesis typical of adipocyte differentiation. Similar to BM-MSC, O-ASC1 cells were capable of accumulating large lipid droplets, whereas O-ASC2 cells tended to uniformly accumulate smaller lipid droplets. Following osteogenic induction, O-ASC1 and to a lesser degree O-ASC2, formed mineral deposits detected with Alziran red (Supplementary Fig. S1) and expressed alkaline phosphatase indicating osteoblastic differentiation. Upon chondrogenic induction, Toluidine Blue staining of sections from pellets grown in suspension indicated the capacity of O-ASC to differentiate into cartilaginous lineage. Expression of collagen II, although detectable in O-ASC1 and O-ASC2, was lower than in BM-MSC differentiation cultures, suggesting that O-ASC formed primarily fibrocartilage. Combined, these results confirm that O-ASC are indeed MSC from the omentum.

ELISA for cytokines—Stromal cells (O-ASC1, BM-MSC, SC-ASC and WI38) were cultured in 10% FBS α-MEM media. Media was removed at intervals from 1 to 7 days, centrifuged and frozen. ELISA assays were then performed on supernatants by using kits from R&D Systems.

Homing of O-ASC to tumors and in vivo effects on tumor growth

To evaluate *in vivo* effects of O-ASC on endometrial cancer growth, immunodeficient nude mice with human endometrial adenocarcinoma Hec1a xenografts in the upper flank were injected into the lower flanks with low doses (10^5 cells three times weekly) of mesenchymal stromal cells. In this metronomic model based on our previous study (6), the mesenchymal cells are remote from the xenografted tumor and must thus be recruited into the tumors, simulating the off-site recruitment of ASC from regional adipose tissue in human tumors. The impact of O-ASC1, O-ASC2 on Hec1a xenograft growth was then compared to SC-ASC and BM-MSC as well as control lung fibroblasts (WI38) and a PBS control group in this metronomic model. Stromal cells injected into lower flank were labeled with GFP or RFP to track engraftment of cells into Hec1a tumors.

Weekly tumor volume measurements demonstrated that Hec1a xenograft growth was significantly ($p<0.05$) accelerated by administration of O-ASC1, O-ASC2, and BM-MSC, as compared with PBS controls (Fig. 2A). In contrast, tumors grown in mice injected with SC-ASC or WI38 did not grow significantly more rapidly than PBS-injected control tumors.

To determine whether the effect of O-ASC on tumor growth could be attributed to more efficient migration of stromal cells into the tumor microenvironment, we evaluated tissue sections to assess biodistribution of injected cells with immunoflouresence to RFP and GFP. Consistent with published studies (6), no GFP+ or RFP+ cells were detected in liver, pancreas, spleen, and other control organs (data not shown). In contrast, comparable numbers of GFP+ or RFP+ cells were detected in tumors of mice administered with O-ASC1, O-ASC2, BM-MSC, and SC-ASC but not WI38. The marker-expressing cells were detected both in the internal zone of the tumor and, more commonly, in the stromal capsule at the tumor periphery (Fig. 2B). Based on the numbers of cells counted in the tumor section area, and the inferred number of such sections composing each tumor, we estimated that on the average 10,000 to 15,000 cells were detectable within a tumor, which corresponds to 10–15% of each injection dose. These numbers, consistent with those reported previously for MSC tumor homing (30), indicate efficient recruitment of administered cells by tumors, but not by normal organs. Lack of tumor growth promotion by SC-ASC despite their capacity for tumor homing indicate that properties unique for O-ASC and BM-MSC are responsible the tumor growth advantage observed upon recruitment of these cells.

We tested the administered cells contribute to the tumor vasculature. Immunofluorescence of tumor sections with antibody recognizing human and mouse CD31 demonstrate that engrafted GFP+ cells are CD31-negative, although often associated with CD31-positive endothelium (Supplementary Fig. S2). This indicates that mesenchymal cells do not transdifferentiate into endothelial cells in this experimental setting. We also did not detect expression of CD34 in engrafted GFP+ cells by using antibodies recognizing human CD34. This is consistent with in vitro flow cytometry analysis of O-ASC demonstrating they were negative for CD34 (Fig. 1).

Effect of O-ASC on tumor matrix organization and cell viability

To investigate the mechanism through which O-ASC promote tumor growth, we analyzed the morphology of fixed tumors recovered in the end of the study. Masson's Trichrome staining for ECM proteins revealed differences in organization of tumors with recruited O-

ASC1, O-ASC2, and BM-MSC as compared with the other groups and control tumors in PBS-injected mice (Fig. 3). The former had thicker peripheral tumor capsule with defined extracellular matrix (ECM) representation (blue) as well as dense inner tumor mass all the way to the center of the tumor core. In contrast, tumors in mice injected with PBS had a thinner peripheral tumor capsule (Fig. 3). Histological analysis also demonstrated that tumors in mice injected with O-ASC1 and O-ASC2 had no detectable necrosis at the tumor periphery and only limited areas of necrosis in the center (Fig. 3). In contrast, the other groups had tumors displaying vast areas of necrosis (detectable as pink areas missing nucleated cells) both at the periphery and particularly in the tumor center. The percentage of tumor containing necrotic areas was quantified to be significantly lower (average of 22% and 9% necrotic tumor area in Hec1a xenografts recruiting O-ASC1 and O-ASC2 as compared to 48% necrotic tumor area in PBS control tumors, $p < 0.05$, Supplementary Fig. S3). These results indicate that O-ASC support the formation of the fibrous tumor capsule and decrease the extent of intra-tumoral necrosis.

Effect of O-ASC on cancer cell proliferation

To determine whether O-ASC promote malignant cell proliferation, we performed immunofluorescence to detect Ki-67, a protein expressed in dividing cells. Immunofluorescence demonstrated that malignant cells throughout the tumors of mice recruiting O-ASC1 and O-ASC2 were almost uniformly positive for Ki-67, while in WI38 and PBS control groups, proliferative tumor cells were limited to the sub-capsular region (Fig. 4A). Quantification of tumor section area containing proliferating cells revealed a higher percentage of proliferative tumor mass in O-ASC1 and O-ASC2 groups, as compared with PBS injected control mice (average of 56% and 88% proliferative tumor mass in O-ASC 1 and O-ASC2 recruiting tumors respectively as compared to 22% for control PBS tumors, $p < 0.05$ Supplementary Fig. S3). The frequency of proliferating cells for tumors recruiting SC-ASC was not significantly higher than PBS control tumors (Fig. 4A and S3).

To test whether the cells recruited by tumors have a direct mitogenic effect on malignant cells, we analyzed proliferation of Hec1a culture *ex-vivo* (Supplementary Fig. S4). In this experiment, luciferase-labeled Hec1a cells were grown with and without O-ASC1, O-ASC2, BM-MSC, SC-ASC or WI38 fibroblasts and tumor cell proliferation was monitored with luciferase imaging. While co-culture with either O-ASC1 or O-ASC2 significantly increased HEC1a cell proliferation, SC-ASC and WI38 control cells had a comparable effect, while BM-MSC on the contrary inhibited Hec1a proliferation. This lack of correlation between the *ex-vivo* and *in-vivo* effects of administered cells on Hec1a suggested that increased proliferation in tumors was likely due to indirect effects of O-ASC.

Effect of O-ASC on tumor vascularization

Blood vessels are essential for tumor oxygenation and nutrient supply, and their deficiency or inefficiency can limit tumor perfusion and growth (31). We therefore investigated whether enhanced angiogenesis could account for the effect of O-ASC on xenograft growth. Interestingly, immunofluorescence with antibodies against CD31 (PECAM-1) or VCAM-1 revealed only weak level of expression of these endothelial makers on many Hec1a xenograft structures that morphologically appeared as vasculature. Nevertheless, CD31 immunofluorescence signal was sufficient for us to detect higher density of vasculature in tumors observed for mice administered with O-ASC1, O-ASC2 and BM-MSC as compared with controls and the other groups (Fig. 4). According to quantification studies, in O-ASC2 groups the percentage of tumor area containing CD31-positive blood vessels was significantly higher than in PBS controls, and there was also a trend for increased vascularization in the O-ASC1 and MSC groups (Supplementary Fig. S3). While large tortuous blood vessels were numerous both at the periphery of the tumor closer to the

capsule (Fig. 4A) and in the core of the tumor (Fig. 4B) for the O-ASC1, O-ASC2 and BM-MSC groups, virtually no CD31-positive vessels were detected in the tumor center for SC-ASC, WI38 and PBS control groups. Similar results were obtained by immunohistochemistry with antibodies against CD34, which stain both endothelial and some of the perivascular/stromal cells (data not shown).

According to the histological evaluation of tumors, the tumors that recruited O-ASC1, O-ASC2 and BM-MSC had a more extensive fibrovascular network and appeared to contain more mature vasculature. The mesenchymal cells within this network are known to be a mixed population of leukocytes and mesenchymal cells, some of which functionally integrate into tumor blood vessels as pericytes and contribute to vascular perfusion capacity (32). To compare the extent of vasculature maturation in tumors recruiting different types of MSC, we analyzed tumor sections for expression of desmin, a marker of pericytes (33). Anti-desmin immunofluoresence revealed robust pericyte coverage throughout the tumor vasculature in mice administered with O-ASC1 and O-ASC2, and to a slighter less extent with BM-MSC and SC-ASC (Fig. 5). Quantification analysis enumerating both perivascular and stromal desmin-positive cells indicated a significant increase in their recruitment, for all groups receiving cell injections, as compared with PBS-injected mice. Mice that received O-ASC1 and O-ASC2 injections had significantly more desmin-positive cells in tumors (Supplementary Fig. S3), consistent with their increased vascularization. Desmin expression was abundant on perivascular cells in large tortuous blood vessels both in sub-capsular layers (Fig. 5A) and in the center (Fig. 5B) of the tumors in mice injected with O-ASC1, O-ASC2 or BM-MSC. In contrast, tumors in mice injected with for SC-ASC and WI38 contained predominantly disseminated desmin-positive cells, while only some areas of the tumor contained rare desmin-positive cells in the PBS group (Fig. 5A,B). Because no clear endothelial networks were revealed with CD31 (Fig. 4) or VCAM-1 (not shown) immunofluorescence in these three groups, it is not clear if these individual desmin-positive cells are associated with abnormal microvasculature weakly expressing endothelial markers or are simply disseminated throughout the stroma. Combined, these observations suggest that O-ASC promote formation of pericyte-coverage and, therefore, likely functional blood vessels throughout the tumor upon recruitment, which explains improved cell survival and proliferation.

Cross-talk between O-ASC and tumor cells

To investigate the potential differences in distinct ASC types to secrete factors known to promote cancer progression, we performed ELISA assays (Supplementary Fig. S5). Conditioned media were analyzed for the concentration of secreted VEGF-A, FGF-2 and HGF. SDF1-alpha (SDF1-α) secretion was analyzed in parallel, as HEC1a tumors secrete CXCR4 and had been shown to respond to SDF1-α. Our data demonstrate that significantly higher levels of VEGF, FGF and SDF1-α are secreted by BM-MSC and O-ASC, as compared to SC-ASC and WI38. These findings suggest that O-ASC and BM-MSC promote tumor growth above the level observed for SC-ASC due to the combined activity of several factors that can directly or indirectly enhance angiogenesis.

Finally, to determine if O-ASC exhibit enhanced in-vitro migration in response to Hec1a secreted factors, we performed an ex-vivo migration assay. The effect of Hec1a-conditioned medium on the motility of cells used in the study was tested by using the Boyden chamber Transwell assay (Supplementary Fig. S6). O-ASC1, O-ASC2 and BM-MSC, but not SC-ASC and WI38 fibroblasts exhibited significant in vitro migration activation in response to Hec1a secreted factors ($p<0.05$). Because the cells responding to tumor signals appear to also be comparatively more efficient in supporting tumors, our data collectively suggest that the cross-talk between malignant and mesenchymal stromal cells is an important component of cancer progression. To gain insight into the potential mechanisms of ASC trafficking to

the tumor, we profiled chemokine secretion by tumor cells. Among a panel of 31 human chemokines tested, we identified IL8 and CXCL1, as chemotactic proteins secreted by Hec1a cells (Supplementary Fig. S7). To determine if these factors could be mechanistically involved in O-ASC migration, we investigated expression of the IL-8 and CXCL1 receptors, CXCR1 and CXCR2, on stromal cells. High levels of CXCR1 expression were detected on O-ASC1, O-ASC2 and BM-MSC, but not on SC-ASC or WI38 fibroblasts (Supplementary Fig. S8), whereas CXCR2 was expressed on all stromal cells investigated. These findings suggest that IL-8 and CXCL1 secretion by Hec1a cells may trigger chemotaxis of stromal cells toward tumors via CXCR1 and CXCR2. Because all cell types displayed tumor homing, we propose that the ubiquitously expressed CXCR2 is responsible for engraftment of the injected cells in our experiment.

Discussion

Mechanism of endometrial tumor growth promotion by O-ASC

Activation and proliferation of stromal cells recruited by tumors leads to their conversion into myofibroblasts/reactive stroma (12, 34, 35). The resulting remodeling of the extracellular matrix (ECM) executed by mesenchymal tumor cells and the resulting desmoplasia is an integral component of cancer progression (36). However, the origins of these stromal cells, which compose the tumor microenvironment and their individual roles in cancer progression, are not well understood. This is due largely to the absence of any specific marker to identify the origins of stromal cells within tumors.

Studies in animal models have demonstrated that upon tumor infiltration, MSC contribute to the CAF pool and establish a trophic microenvironment (11, 37). In previous studies by us and others, MSC have been shown to traffic to tumors (19, 30) and participate in forming the supportive fibrovascular network (33, 38–40). While there is evidence that cells composing tumor stroma can be recruited from the bone marrow, their possible extramedullary origins have been less well explored. Adipose tissue is particularly rich in MSC and could thus serve as primary MSC source for tumors (7, 41). While systemic mobilization of MSC from adipose tissue (ASC) has been proposed (25, 26, 42) and recruitment of ASC from remote depots is conceivable and has been shown to occur in mouse cancer models(6), it is likely that adipose tissue adjacent to the tumor may be a more significant contributor of ASC. Moreover, the differences reported for ASC residing in subcutaneous and visceral adipose depots (43) suggest that ASC from the omentum could have a distinct role in the progression of intraperitoneal cancers.

Here, we analyzed omental adipose tissue, which is the primary intraperitoneal reservoir of adipose tissue which is routinely removed during staging procedures for endometrial and ovarian cancer (44). This is the first study investigating the effects of omental derived adipose stem cells on cancer progression. We found that O-ASC from different patients exhibit morphology, cell surface marker expression, and differentiation capacity comparable to those observed for BM-MSC and previously reported for SC-ASC (45). O-ASC, SC-ASC, and BM-MSC exhibited tumor tropism when injected into tumor-bearing mice distantly from the endometrial xenograft. Despite these similarities, we found that O-ASC had more potent effect than SC-ASC on endometrial cancer cell proliferation and survival *in-vivo*, thus resulting in expedited tumor growth. O-ASC and SC-ASC were isolated from donors with comparable BMI, suggesting that the differences in their cancer promotion capacity cannot be attributed to obesity-associated changes in ASC properties. Consistent with promoted angiogenesis being the foundation of increased tumor cell mass (31), O-ASC recruitment correlated with higher abundance of both small and large tortous blood vessels suggesting that O-ASC tumor homing promotes the vascularization of endometrial caners. In addition, we observed increased pericyte coverage of vasculature in tumors recruiting O-

ASC. Accumulating evidence indicates that ASC serve as pericytes in adipose tissue (46), which could be their function uncoupled from multipotency and capacity to serve as progenitor cells. While our previous studies show that ASC can acquire perivascular localization upon tumor homing, the numbers of administered O-ASC observed in the tumors cannot account for the increased numbers of desmin-positive cells. Therefore, O-ASC may play a role in recruiting endogenous pericyte progenitors that contribute to the formation of functional tumor vessels.

Increased microvascular density (MVD) has been associated with advanced stage and poor prognosis in endometrial cancer (47, 48). In our study there was a clear correlation between the capacity of an administered mesenchymal cell type to enhance tumor vascularization and its mitogenic and necrosis-protective effects. These findings suggest that O-ASC promote tumor growth through stimulation of angiogenesis. While these findings are consistent with the previously reported pro-angiogenic ASC properties (46), they for the first time suggest that visceral adipose tissue contains a population of MSC with unique tumor promoting qualities. Our data indicate VEGF, FGF and SDF1-α as candidate molecules responsible for the superior capacity of O-ASC to promote tumor growth. Future studies systematically surveying secretomes of ASC from distinct WAT depots may identify new tumorigenic factors synergizing with VEGF, FGF and SDF1-α.While the vasculogenic function of O-ASC may be sufficient to explain their tumor growth-promoting effects in our study, it is not clear why BM-MSC had a comparable effect on tumor growth despite their comparatively lower effect on the promotion of tumor vascularization. The mechanisms through which stromal cells regulate tumor physiology are complex and multifaceted, and their functions independent of angiogenesis regulation are likely to play a role. In addition to their direct pro-angiogenic properties, MSC execute their function through the production of collagens and other ECM proteins, which provide the framework of the tumor microenvironment, as well as in resolving scarring during consecutive stages of inflammatory processes (49). Although we could not detect quantifiable differences in the ECM deposition between different groups, stromatogenesis and desmoplasia concomitant with angiogenesis are likely to be important as mechanisms through which O-ASC regulate cancer progression. In addition, recent studies demonstrate the capacity of MSC to induce the epithelial-to-mesenchymal transition (EMT) in malignant cells and promote metastasis(14, 18). The EMT has been shown to activate both proliferation and migration of malignant cells, which makes it interesting to consider possible role of O-ASC in promoting metastatic cancer dissemination. Finally, like other MSC, ASC have been shown to suppress inflammation and mute T cell function (49), which could at least partially account for the increased tumor cell survival observed. There is a possibility that in addition to inducing pericyte recruitment or differentiation, O-ASC could affect the immune response through modulating infiltration of other cell populations from the bone marrow. Because monocytes/macrophages and various lymphocyte populations are known to influence tumor growth, we measured their content in the tumors by immunofluorescence. While we did not detect significant differences in macrophage and lymphocyte content between different animal groups (data not shown) a more detailed analysis may be needed in future studies to comprehensively analyze the role of ASC in shaping the composition of tumor microenvironment.

We identified IL-8 as a potential chemotactic signaling pathway involved in O-ASC recruitment. Chemokine profiling demonstrated that CXCL8 (IL-8) and CXCL1 are secreted by Hec1a endometrial carcinoma cells. The IL-8 receptor, CXCR1, was detected on O-ASC1, O-ASC2 and BM-MSC but not SC-ASC or WI39 cells, suggesting a role for IL-8 signaling in O-ASC recruitment and possibly tumor promotion. IL8 has previously been reported to support MSC recruitment in a glioma model and to mediate radiation-enhanced tumor tropism of MSC(50–52). Future studies will investigate the therapeutic potential of

inhibiting O-ASC recruitment by suppressing signaling through chemotactic pathways such as IL-8.

In summary, our results show that the omentum contains a population of MSC which resemble BM-MSC and SC-ASC with regard to cell surface marker expression and multipotency but have a unique effect on tumor progression, suggesting their role in etiology of human intraperitoneal cancers. Our combined data indicate that O-ASC support tumor vascularization, which leads to enhanced survival and proliferation of malignant cells and may contribute to O-ASC effects on tumor growth. We propose that the cross talk between the tumor and the surrounding adipose tissue could contribute to ASC "education" and their adaptation for the tumor benefit, thus resulting in a "vicious circle" driving the progression of cancer. Our findings suggest a novel mechanism accounting for the increased risk and mortality of endometrial cancer in women with excess visceral adipose tissue. Preventing migration of O-ASC into endometrial cancers by disrupting interactions of O-ASC with malignant cells, tumor endothelium and other tumor stromal cells may be a novel treatment strategy.

Supplementary Material

Refer to Web version on PubMed Central for supplementary material.

Acknowledgments

Support for KL and RB from NIH 2P50 CA098258-06 SPORE; for KM from Komen KG080782 and NIH P50 CA140388 SPORE.

We thank Chieh Tseng for technical help in tissue analysis.

References

1. Flegal KM, Graubard BI, Williamson DF, Gail MH. Cause-specific excess deaths associated with underweight, overweight, and obesity. JAMA. 2007; 298:2028–37. [PubMed: 17986696]
2. Calle EE, Rodriguez C, Walker-Thurmond K, Thun MJ. Overweight, obesity, and mortality from cancer in a prospectively studied cohort of U.S. adults. N Engl J Med. 2003; 348:1625–38. [PubMed: 12711737]
3. Friedenreich C, Cust A, Lahmann PH, Steindorf K, Boutron-Ruault MC, Clavel-Chapelon F, et al. Anthropometric factors and risk of endometrial cancer: the European prospective investigation into cancer and nutrition. Cancer Causes Control. 2007; 18:399–413. [PubMed: 17297555]
4. Bergstrom A, Pisani P, Tenet V, Wolk A, Adami HO. Overweight as an avoidable cause of cancer in Europe. Int J Cancer. 2001; 91:421–30. [PubMed: 11169969]
5. Basen-Engquist K, Chang M. Obesity and cancer risk: recent review and evidence. Curr Oncol Rep. 13:71–6. [PubMed: 21080117]
6. Zhang Y, Daquinag A, Traktuev DO, Amaya F, Simmons PJ, March KL, et al. White adipose tissue cells are recruited by experimental tumors and promote cancer progression in mouse models. Cancer Res. 2009; 69:5259–66. [PubMed: 19491274]
7. Dominici M, Le Blanc K, Mueller I, Slaper-Cortenbach I, Marini F, Krause D, et al. Minimal criteria for defining multipotent mesenchymal stromal cells. The International Society for Cellular Therapy position statement. Cytotherapy. 2006; 8:315–7. [PubMed: 16923606]
8. Daquinag AC, Zhang Y, Kolonin MG. Vascular targeting of adipose tissue as an anti-obesity approach. Trends Pharmacol Sci. 32:300–7. [PubMed: 21349592]
9. Galie M, Konstantinidou G, Peroni D, Scambi I, Marchini C, Lisi V, et al. Mesenchymal stem cells share molecular signature with mesenchymal tumor cells and favor early tumor growth in syngeneic mice. Oncogene. 2007; 27:2542–5. [PubMed: 17998939]

10. Hu M, Yao J, Carroll DK, Weremowicz S, Chen H, Carrasco D, et al. Regulation of in situ to invasive breast carcinoma transition. Cancer Cell. 2008; 13:394–406. [PubMed: 18455123]
11. Orimo A, Weinberg RA. Stromal fibroblasts in cancer: a novel tumor-promoting cell type. Cell Cycle. 2006; 5:1597–601. [PubMed: 16880743]
12. Baglole CJ, Ray DM, Bernstein SH, Feldon SE, Smith TJ, Sime PJ, et al. More than structural cells, fibroblasts create and orchestrate the tumor microenvironment. Immunol Invest. 2006; 35:297–325. [PubMed: 16916756]
13. Hall B, Dembinski J, Sasser AK, Studeny M, Andreeff M, Marini F. Mesenchymal stem cells in cancer: tumor-associated fibroblasts and cell-based delivery vehicles. Int J Hematol. 2007; 86:8–16. [PubMed: 17675260]
14. Karnoub AE, Dash AB, Vo AP, Sullivan A, Brooks MW, Bell GW, et al. Mesenchymal stem cells within tumour stroma promote breast cancer metastasis. Nature. 2007; 449:557–63. [PubMed: 17914389]
15. Zhu W, Boachie-Adjei O, Rawlins BA, Frenkel B, Boskey AL, Ivashkiv LB, et al. A novel regulatory role for stromal-derived factor-1 signaling in bone morphogenic protein-2 osteogenic differentiation of mesenchymal C2C12 cells. J Biol Chem. 2007; 282:18676–85. [PubMed: 17439946]
16. Djouad F, Plence P, Bony C, Tropel P, Apparailly F, Sany J, et al. Immunosuppressive effect of mesenchymal stem cells favors tumor growth in allogeneic animals. Blood. 2003; 102:3837–44. [PubMed: 12881305]
17. Djouad F, Mrugala D, Noel D, Jorgensen C. Engineered mesenchymal stem cells for cartilage repair. Regen Med. 2006; 1:529–37. [PubMed: 17465847]
18. Klopp AH, Lacerda L, Gupta A, Debeb BG, Solley T, Li L, et al. Mesenchymal stem cells promote mammosphere formation and decrease E-cadherin in normal and malignant breast cells. PLoS One. 5:e12180. [PubMed: 20808935]
19. Klopp AH, Spaeth EL, Dembinski JL, Woodward WA, Munshi A, Meyn RE, et al. Tumor irradiation increases the recruitment of circulating mesenchymal stem cells into the tumor microenvironment. Cancer Res. 2007; 67:11687–95. [PubMed: 18089798]
20. Prizment AE, Flood A, Anderson KE, Folsom AR. Survival of women with colon cancer in relation to precancer anthropometric characteristics: the Iowa Women's Health Study. Cancer Epidemiol Biomarkers Prev. 19:2229–37. [PubMed: 20826830]
21. Balentine CJ, Enriquez J, Fisher W, Hodges S, Bansal V, Sansgiry S, et al. Intra-abdominal fat predicts survival in pancreatic cancer. J Gastrointest Surg. 14:1832–7. [PubMed: 20725799]
22. Nie J, Chang B, Traktuev DO, Sun J, March KL, Chan L, et al. Combinatorial peptides identify α5β1 integrin as a receptor for the matricellular protein SPARC on adipose stromal cells. Stem Cells. 2008; 26:2735–45. [PubMed: 18583538]
23. Pittenger MF, Mackay AM, Beck SC, Jaiswal RK, Douglas R, Mosca JD, et al. Multilineage potential of adult human mesenchymal stem cells. Science. 1999; 284:143–7. [PubMed: 10102814]
24. Bakker AH, Van Dielen FM, Greve JW, Adam JA, Buurman WA. Preadipocyte number in omental and subcutaneous adipose tissue of obese individuals. Obes Res. 2004; 12:488–98. [PubMed: 15044666]
25. Kolonin MG, Simmons PJ. Combinatorial stem cell mobilization. Nat Biotechnol. 2009; 27:252–3. [PubMed: 19270674]
26. Bellows CF, Zhang Y, Simmons PJ, Khalsa AS, Kolonin MG. Influence of BMI on Level of Circulating Progenitor Cells. Obesity. 2011; 19:1722–6. [PubMed: 21293449]
27. Lois C, Hong EJ, Pease S, Brown EJ, Baltimore D. Germline transmission and tissue-specific expression of transgenes delivered by lentiviral vectors. Science. 2002; 295:868–72. [PubMed: 11786607]
28. Bianco P, Robey PG, Simmons PJ. Mesenchymal stem cells: revisiting history, concepts, and assays. Cell Stem Cell. 2008; 2:313–9. [PubMed: 18397751]
29. Dominici M, Le Blanc K, Mueller I, Slaper-Cortenbach I, Marini F, Krause D, et al. Minimal criteria for defining multipotent mesenchymal stromal cells. The International Society for Cellular Therapy position statement. Cytotherapy. 2006; 8:315–7. [PubMed: 16923606]

30. Kidd S, Spaeth E, Dembinski JL, Dietrich M, Watson K, Klopp A, et al. Direct evidence of mesenchymal stem cell tropism for tumor and wounding microenvironments using in vivo bioluminescent imaging. Stem Cells. 2009; 27:2614–23. [PubMed: 19650040]
31. Hanahan D, Weinberg RA. Hallmarks of cancer: the next generation. Cell. 2011; 144:646–74. [PubMed: 21376230]
32. Du R, Lu KV, Petritsch C, Liu P, Ganss R, Passegue E, et al. HIF1alpha induces the recruitment of bone marrow-derived vascular modulatory cells to regulate tumor angiogenesis and invasion. Cancer Cell. 2008; 13:206–20. [PubMed: 18328425]
33. Spaeth EL, Dembinski JL, Sasser AK, Watson K, Klopp A, Hall B, et al. Mesenchymal stem cell transition to tumor-associated fibroblasts contributes to fibrovascular network expansion and tumor progression. PLoS One. 2009; 4:e4992. [PubMed: 19352430]
34. Dvorak HF. Tumors: wounds that do not heal. Similarities between tumor stroma generation and wound healing. N Engl J Med. 1986; 315:1650–9. [PubMed: 3537791]
35. Coussens LM, Werb Z. Inflammation and cancer. Nature. 2002; 420:860–7. [PubMed: 12490959]
36. Bissell MJ, Radisky D. Putting tumours in context. Nat Rev Cancer. 2001; 1:46–54. [PubMed: 11900251]
37. Galie M, Konstantinidou G, Peroni D, Scambi I, Marchini C, Lisi V, et al. Mesenchymal stem cells share molecular signature with mesenchymal tumor cells and favor early tumor growth in syngeneic mice. Oncogene. 2008; 27:2542–51. [PubMed: 17998939]
38. Hall B, Dembinski J, Sasser AK, Studeny M, Andreeff M, Marini F. Mesenchymal stem cells in cancer: tumor-associated fibroblasts and cell-based delivery vehicles. Int J Hematol. 2007; 86:8–16. [PubMed: 17675260]
39. Nakamizo A, Marini F, Amano T, Khan A, Studeny M, Gumin J, et al. Human bone marrow-derived mesenchymal stem cells in the treatment of gliomas. Cancer Res. 2005; 65:3307–18. [PubMed: 15833864]
40. Studeny M, Marini FC, Dembinski JL, Zompetta C, Cabreira-Hansen M, Bekele BN, et al. Mesenchymal stem cells: potential precursors for tumor stroma and targeted-delivery vehicles for anticancer agents. J Natl Cancer Inst. 2004; 96:1593–603. [PubMed: 15523088]
41. Zuk PA, Zhu M, Mizuno H, Huang J, Futrell JW, Katz AJ, et al. Multilineage cells from human adipose tissue: implications for cell-based therapies. Tissue Eng. 2001; 7:211–28. [PubMed: 11304456]
42. Bellows CF, Zhang Y, Chen J, Frazier ML, Kolonin MG. Circulation of progenitor cells in obese and lean colorectal cancer patients. Cancer Epidemiol Biomarkers Prev. 2011; 20:2461–8. [PubMed: 21930958]
43. Joe AW, Yi L, Even Y, Vogl AW, Rossi FM. Depot-specific differences in adipogenic progenitor abundance and proliferative response to high-fat diet. Stem Cells. 2009; 27:2563–70. [PubMed: 19658193]
44. Usubutun A, Ozseker HS, Himmetoglu C, Balci S, Ayhan A. Omentectomy for gynecologic cancer: how much sampling is adequate for microscopic examination? Arch Pathol Lab Med. 2007; 131:1578–81. [PubMed: 17922596]
45. Suga H, Shigeura T, Matsumoto D, Inoue K, Kato H, Aoi N, et al. Rapid expansion of human adipose-derived stromal cells preserving multipotency. Cytotherapy. 2007; 9:738–45. [PubMed: 18058361]
46. Traktuev D, Merfeld-Clauss S, Li J, Kolonin M, Arap W, Pasqualini R, et al. A Population of multipotent CD34-positive adipose stromal cells share pericyte and mesenchymal surface markers, reside in a periendothelial location, and stabilize endothelial networks. Circ Res. 2008; 102:77–85. [PubMed: 17967785]
47. Kamat AA, Merritt WM, Coffey D, Lin YG, Patel PR, Broaddus R, et al. Clinical and biological significance of vascular endothelial growth factor in endometrial cancer. Clin Cancer Res. 2007; 13:7487–95. [PubMed: 18094433]
48. Espinosa I, Jose Carnicer M, Catasus L, Canet B, D'Angelo E, Zannoni GF, et al. Myometrial invasion and lymph node metastasis in endometrioid carcinomas: tumor-associated macrophages, microvessel density, and HIF1A have a crucial role. Am J Surg Pathol. 34:1708–14. [PubMed: 20962622]

49. Caplan AI. Adult mesenchymal stem cells for tissue engineering versus regenerative medicine. J Cell Physiol. 2007; 213:341–7. [PubMed: 17620285]

50. Halpern JL, Kilbarger A, Lynch CC. Mesenchymal stem cells promote mammary cancer cell migration in vitro via the CXCR2 receptor. Cancer Lett. 2011; 308:91–9. [PubMed: 21601983]

51. Birnbaum T, Roider J, Schankin CJ, Padovan CS, Schichor C, Goldbrunner R, et al. Malignant gliomas actively recruit bone marrow stromal cells by secreting angiogenic cytokines. J Neurooncol. 2007; 83:241–7. [PubMed: 17570034]

52. Kim SM, Oh JH, Park SA, Ryu CH, Lim JY, Kim DS, et al. Irradiation enhances the tumor tropism and therapeutic potential of tumor necrosis factor-related apoptosis-inducing ligand-secreting human umbilical cord blood-derived mesenchymal stem cells in glioma therapy. Stem Cells. 2010; 28:2217–28. [PubMed: 20945331]

Translational Relevance

Both incidence and progression of endometrial cancer is positively associated with obesity. Preferential distribution of adipose tissue in the abdomen further increases the risk of endometrial cancer, as well as the risk and mortality of other intra-abdominal cancers. We hypothesized that visceral adipose tissue contains a population of tumor-promoting stromal progenitors to account for the link between visceral obesity and malignancy. To investigate this, we isolated and characterized adipose stromal cells from the omentum of two patients with gynecologic cancer (O-ASC). Using an endometrial cancer xenograft model, we compared the effects of O-ASC and subcutaneous ASC (SC-ASC) on cancer progression. O-ASC more potently facilitated tumor growth and enhanced tumor vascularization. Our data indicate that O-ASC and SC-ASC are equally efficient in homing to tumors but are markedly different in their function. These findings suggest that excess visceral adipose tissue promotes malignancy by providing mesenchymal stromal cells to intra-abdominal tumors, and thus may represent a new therapeutic target.

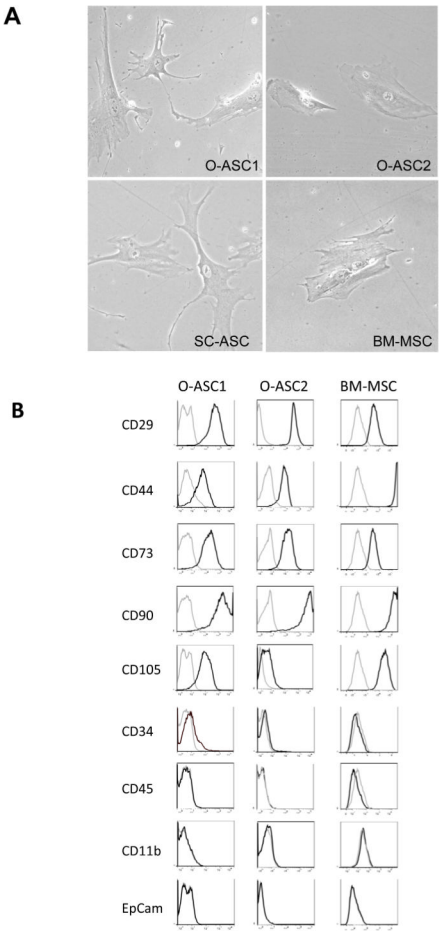

Figure 1.
Characterization of O-ASC. (A) Morphology of adherent cells demonstrating similarity of O-ASC to SC-ASC and BM-MSC. (B) Flow cytometric characterization of O-ASC based on surface marker expression indicates their similarity to BM-MSC. Light gray lines: isotype controls.

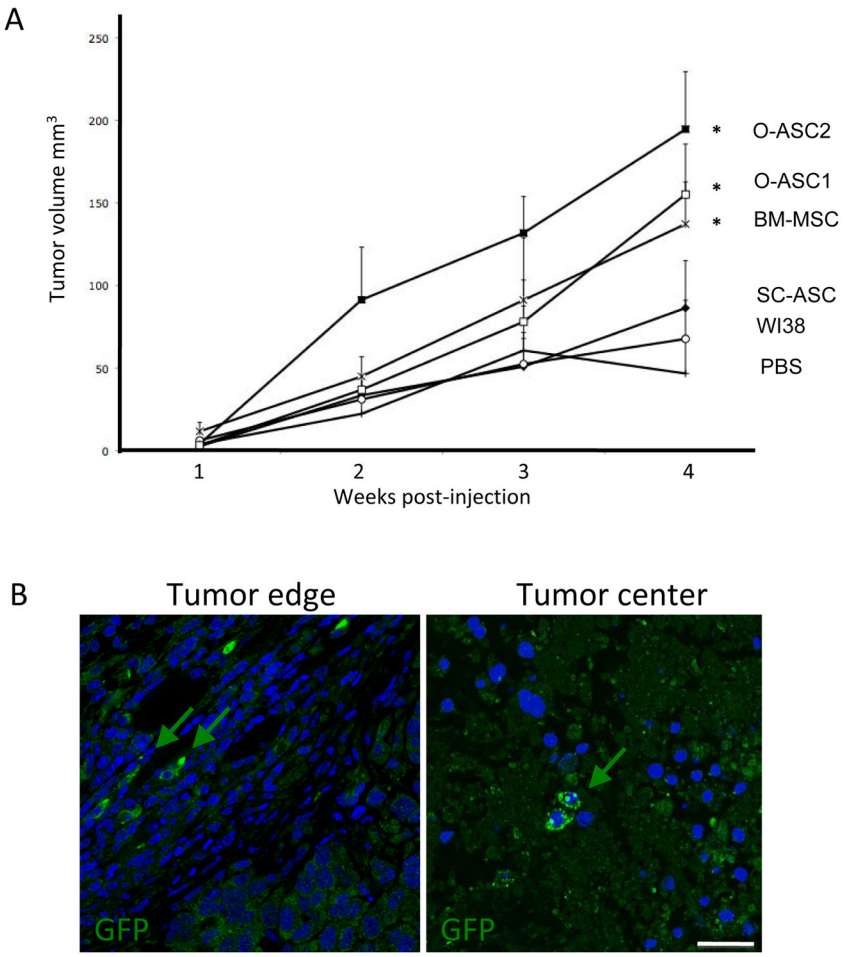

Figure 2.

Experimental endometrial tumor growth promotion by O-ASC. (A) Nude mice xenografted (at week 0) with Hec1a tumors have been subcutaneously injected (lower back) starting 1 day post-xenografting with O-ASC, SC-ASC, BM-MSC, WI38 fibroblasts or PBS on alternating sides 3 times a week. N=5 / group. O-ASC1, O-ASC2 and BM-MSC significantly increase xenograft growth (* $p<0.05$ compared to PBS group, Student's *t* test). Error bars: SEM. (B) Homing of injected cells detected by immunofluorescence analysis of paraffin sections of tumors collected in the end of the injection cycle with anti-GFP antibodies. Green arrows indicate cells engrafted in tumor peripheral and central compartments. Nuclei are stained blue. Scale bar: 50 μM.

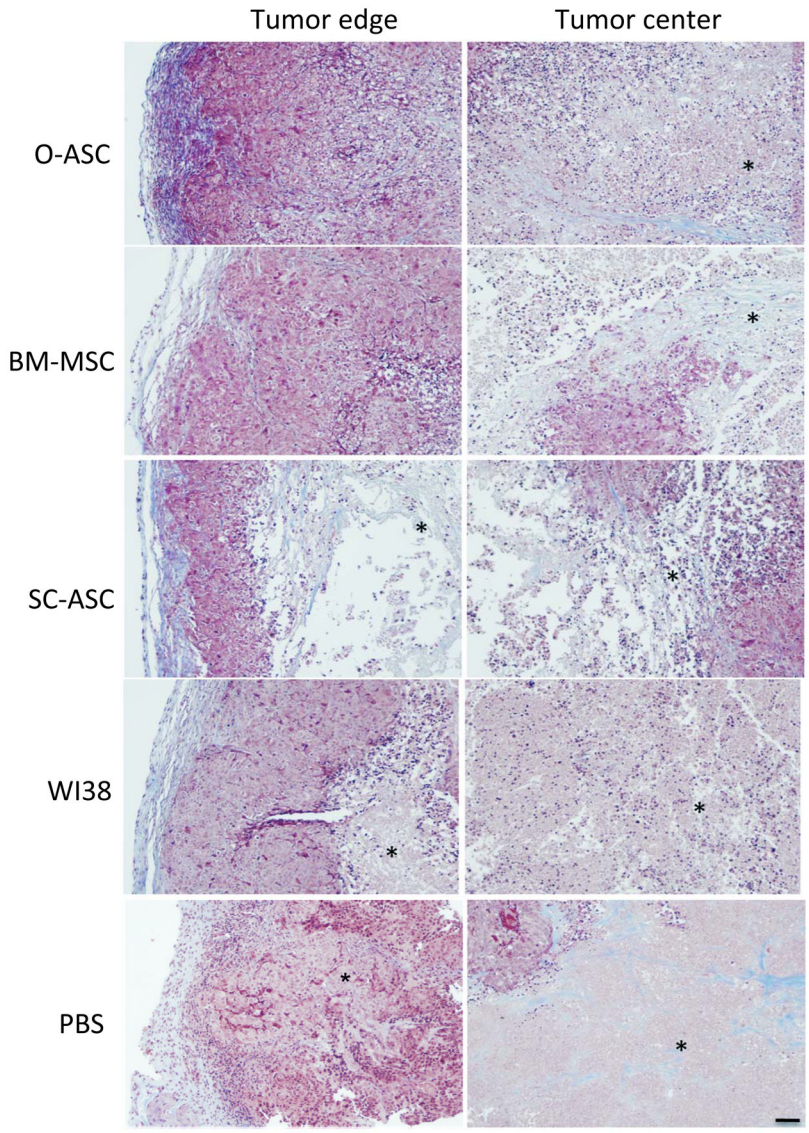

Figure 3.

Histological tumor analysis. Masson's Trichrome staining of sections of tumors collected in the end of the injection cycle reveals increased capsular ECM deposition (blue), higher density of viable cells (dark purple nuclei) and lack of anucleated necrotic areas (*) in both peripheral and inner compartments of tumors recruiting O-ASC. This is contrasted with control tumors, which exhibited less capsular ECM deposition in the capsule with increased central tumor necrosis. Scale bar: 500 μM.

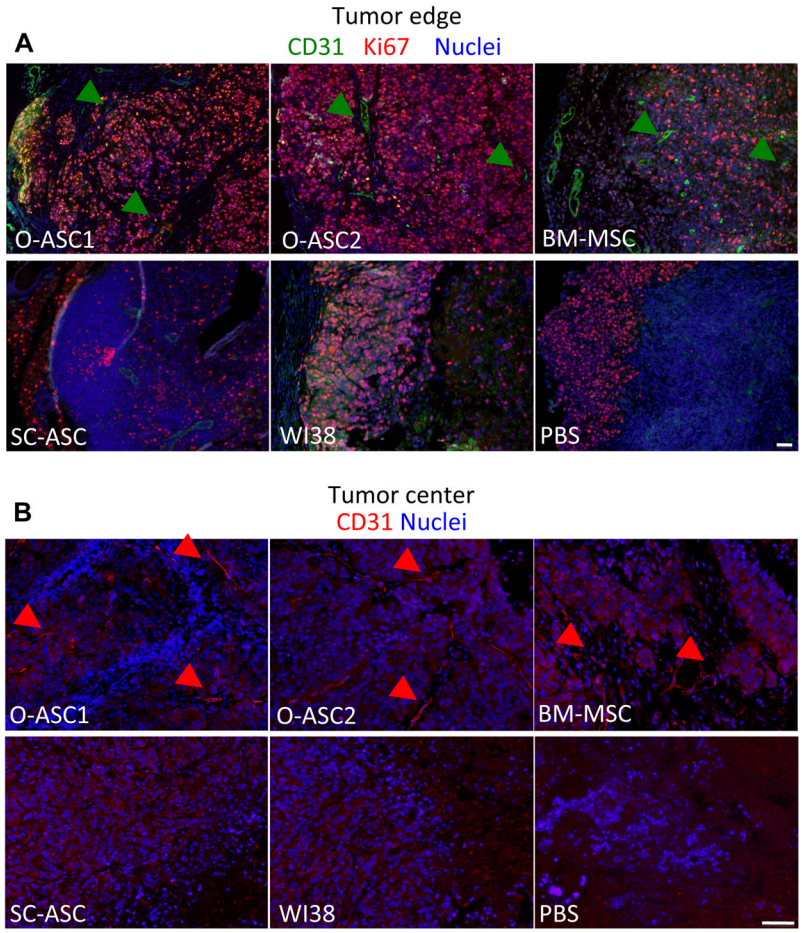

Figure 4.

Tumor cell proliferation and vascularization. Immunofluorescence analysis of sections of tumors collected in the end of the injection cycle. (A) Edge of the tumor (left) and proximal layers stained with anti-CD31 (green) and anti-Ki67 (red) antibodies revealing increased density of proliferating cells residing in deeper tumor layers and increased presence of large tortuous blood vessels (arrows). (B) Increased vascularization associated with O-ASC and BM-MSC injection confirmed for inner compartments of tumors. Nuclei are blue. Scale bar: 500 μM.

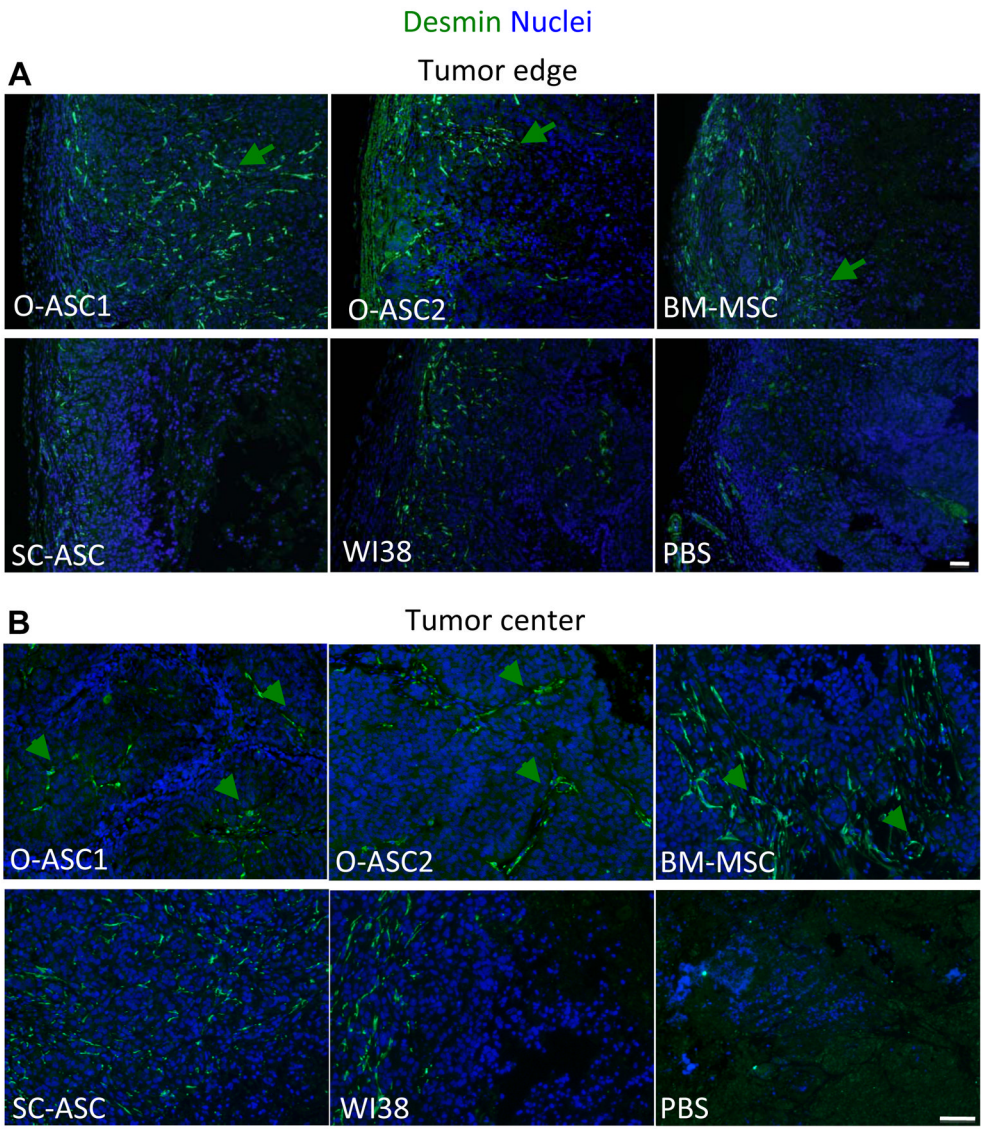

Figure 5.

Tumor vasculature maturity analysis. Immunofluorescence analysis of sections of tumors collected in the end of the injection cycle with anti-desmin (green) antibodies reveals increased density of large tortuous vessels covered with pericytes in both peripheral (A) and inner compartments (B) of tumors recruiting O-ASC or BM-MSC. Serial tumor sections shown in (B) correspond to those stained with CD31 in Figure 4B. Nuclei are blue. Scale bar: 500 μM.